Published: 12th May 2026

ANACHEM JOURNAL
ISSN: 2006-5221 (Online)

GREEN SYNTHESIS OF NANOCHITOSAN USING AFRICAN OIL PALM (*Elaeis Guineensis*) PETIOLE AS DEACETEYLATING AND DEPROTEINATING AGENT

***[1]Obiefuna, J.N., [1]Ezike, C.C., [2]Akinyele, B.A., and [1]Gambo, A.**

[1]Department of Pure and Industrial Chemistry, Nnamdi Azikiwe University, Awka, Anambra State, Nigeria.
[2]Institute of Ecology and Environmental Studies, Obafemi Awolowo University, Ile-lfe, Osun State, Nigeria.
*Corresponding author's e-mail: jn.obiefuna@unizik.edu.ng
DOI: https://doi.org/10.5281/zenodo.20129473

ABSTRACT

Chitosan, a derivative of chitin composed of β-(1→4)-linked 2-acetamido-2-deoxy-D-glucose units, is widely used in environmental, biomedical, and food industries. In this study, chitosan was extracted from periwinkle shells (*Tympanotonus fuscatus*) using alkali obtained from the ash of the petioles of oil palm (*Elaeis guineensis*) petioles, which served as a green agent for deproteination and deacetylation. The extracted chitosan was further reduced to nanochitosan using a sodium tripolyphosphate solution. The proximate analysis and characterization of nanochitosan were conducted using Fourier transform infrared (FTIR), scanning electron microscopy (SEM), transmission electron microscopy (TEM), thermo-gravimetric analysis (TGA), and X-ray diffraction (XRD). The physical properties of the ashed *E. guineensis* extract, determined using standard methods, included the ash content. (17.30%), pH (11.74), yield (76.20%), and alkali content of 0.88 M. Proximate analysis of the chitosan revealed moisture content of 4.43%, ash content 5.26%, protein 1.06%, fat 0.48%, water binding capacity of 1260%, fat binding capacity of 381.30%, and was soluble in 1% acetic acid. The degree of deacetylation was 90.55%, and the percentage yield was 89%. Characterization using FTIR spectra confirmed the presence of functional groups such as –OH, –NH, –$CONH_2$, C=O, and C–H, with peaks ranging from 3779.00-567.00 cm-1. SEM and TEM analyses showed spherical, porous, and agglomerated nanoparticles. The XRD and TGA results indicated that the nanochitosan is semi-crystalline, thermally stable, and non-volatile. Overall, the research demonstrated that nanochitosan was successfully produced using biowaste, yielding a high-quality, low-toxicity chitosan suitable for diverse industrial applications.
Keywords: Characterization; *Elais guineensis*; NanoChitosan; Periwinkle shell; Physico-chemical.

1.0. Introduction

The shells of crustaceans and molluscs discarded during food processing are often present in large quantities and, if not properly managed, can cause environmental and human health problems. However, these wastes can be harnessed to produce highly viable and useful products (Gbenebor et al., 2017). Periwinkle shells are abundant in Nigeria and can be used as a source of chitosan, as they contain varying amounts of chitin and $CaCO_3$, similar to those of other Crustaceans and Molluscs (Gbenebor et al., 2017).

Chitosan is a naturally occurring, biodegradable, and biocompatible polysaccharide derived from chitin, which is abundantly found in the exoskeletons of crustaceans, insects, and fungal cell walls. Structurally, chitosan consists of β-(1→4)-linked D-glucosamine and N-acetyl-D glucosamine units (Thambiliyagodage et al.,

2023). The presence of amino (-NH_2) and hydroxyl (-OH) groups in chitosan's chemical structure is responsible for its specific properties and reactivity. Chitosan is an eco-friendly biopolymer with distinctive qualities, including antimicrobial properties, high adsorption capacity, film-forming ability, and non-toxicity, making it a sustainable alternative to synthetic polymers used in biomedical, food technology, environmental, and pharmaceutical applications (Vega-Baudrit et al., 2025). Traditionally, nanochitosan is produced from chitin via chemical processes that use strong acids (for demineralization) and concentrated alkalis (for deproteination and deacetylation). However, the conventional use of commercial caustic soda for deproteination and deacetylation processes is associated with several drawbacks, including the generation of hazardous waste, degradation of polymer quality, chemical residues in chitosan, and environmental pollution (El-Naggar et al., 2022). Inorganic alkaline solutions are often potent chemical substances with a notable ecological footprint. The manufacture and disposal of these substances can cause pollution, and the handling of highly alkaline inorganic solutions can be hazardous. They can cause chemical burns, eye and skin irritation, and respiratory problems if not properly managed (Agbenorku et al., 2015). These limitations have driven the development of green synthesis approaches that align with the principles of green chemistry, aiming to reduce environmental hazards while maintaining a homogeneous, pure product. Green synthesis approaches have gained significant traction globally, including in Nigeria, by utilizing biological agents such as plant extracts or microorganisms as reducing and stabilizing agents (El-Naggar et al., 2022; Riki et al., 2025). The green synthesis of nanochitosan uses locally available resources, such as agricultural waste or indigenous plants, to produce nanoparticles under mild conditions without the use of toxic chemicals. This approach not only aligns with the principles of green chemistry but also offers economic advantages by reducing costs and supporting local industries.

Oil palm, scientifically known as Elaeis guineensis, is a tropical plant native to West Africa, including the South-East region of Nigeria, and offers socio-economic benefits (Okolo et al., 2019). The potential of oil palm as a source of caustic alkali lies in its biomass, particularly the ash produced by incinerating oil palm waste (empty fruit bunches, palm kernel shells, fronds). The ash is usually rich in potassium, which is leached with water to produce a solution of potassium hydroxide, a caustic alkali (Widiputri et al., 2022). The use of plant-based alkaline extracts in place of conventional inorganic alkaline solutions in the deproteination and deacetylation processes is a commercially viable area to explore. This study aims to use a natural alkali extract from oil palm petioles (*Elaeis guineensis*) as a green deproteination and deacetylation agent for extracting chitosan from periwinkle shells, thereby advancing green chemistry.

2.0. Materials and Methods

Sample collection and preparation: Fresh periwinkle shells (*T. fuscatus*) were collected from the Esuk Itsu riverbank in Urua ato, Ikot Ekpene, Akwa Ibom State, Nigeria. The periwinkle samples were washed, cleaned to remove dirt and other impurities, and later sun-dried for 120 hours, after which they were ground to a fine powder and stored in clean, dry plastic bags at an ambient room temperature of 25 °C.

The petioles of *E. guineensis* were collected from the herbarium of Nnamdi Azikiwe University, Awka, Anambra State. The petioles of the *E. guineensis* husk were rinsed with distilled water, air-dried at room temperature for 120 hours, then ground to a fine powder and ash-washed in an electric furnace at 800 °C for 1 hour until a white ash was obtained.

2.1. Method of Analysis

2.1.1. Extraction of Alkali from petioles of *E. guineensis*: One hundred grams of the ashed E. *guineensis* was poured into a 1 litre beaker containing 800 mL of distilled water. The

resulting ash solution was thoroughly stirred and left at room temperature for 72 hours to maximise alkaline extraction. Finally, the solution was decanted to obtain the alkaline extract (Maliki et al., 2020).

2.1.2. Standardization of the E. *guineensis* Alkali Extracts: Standardization was performed as described by Maliki et al. (2020). 25 mL of the alkali extract was pipetted and titrated against a 1 M hydrochloric acid solution, using methyl orange as an indicator. The titration was performed in triplicate, and the average titre was used to calculate the extract's alkali content at a 1:1 molar ratio.

The equation is represented by: $\frac{M1V1}{M2V2} = Mole\ ratio$

(M_1= Molarity of the acid, M_2 = Molarity of the base, V_1 = Volume of acid, V_2 = Volume of the base. colour at endpoint is orange)

2.2. Chitosan Extraction: The chitosan extraction involves three major steps: demineralization, deproteinization, and deacetylation as prescribed by Obiefuna and Chukwudum, (2024).

2.2.1. Demineralization: The method used was described by Obiefuna and Chukwudum, (2024). Two hundred grams of the ground periwinkle shell was soaked in 4 % HCl at room temperature in the solid-to-solvent ratio of 14:1 (w/v) for 24 hours. It was washed in the acidic solution until the bubbles stopped, with no colour change observed in the mixture. The shell was washed with deionized water until a neutral pH was reached and dried to a constant weight.

2.2.2. Deproteinization and Deacetylation: The method used was adopted from Okafor & Obiefuna (2024). The demineralized powder was treated with 2% standardized caustic natural alkali from *E. guineensis* extracts at a 1:20 (w/v) ratio. The mixture was heated at 90 °C with constant stirring for 2 hours, then filtered under reduced pressure. The residue was washed thoroughly with distilled water until a pH of 7 was reached, and subsequently sun-dried to obtain chitin. The Chitin was further treated with a 40% standardized caustic alkali solution at a 1:15 (w/v) ratio to obtain a mixture, which was filtered using a pump filter. The residue obtained was the extracted chitosan. It was washed with deionized water until neutral pH (7) and then oven-dried at 105 °C for 24 hours to obtain pure chitosan.

2.3. Preparation of Nanochitosan: Two grams of chitosan were first dissolved in 50 mL of 1% v/v acetic acid with constant stirring to obtain a solution. Additionally, 100 mg of sodium tripolyphosphate was dissolved in 100 mL of deionized water, and the resulting solution was added to the chitosan solution dropwise at 1 mL/min for reduction. The mixture was centrifuged at 1000 rpm for 5 minutes. The collected residue was filtered through 0.2 µm filter paper for the nanochitosan.

2.4. Proximate Profile of the Chitosan and Ashed *E. guineensis*: The proximate composition (ash, pH, moisture, protein, and fat) of chitosan and ashed *E. guineensis* was analyzed according to the AOAC (2015) method with some modifications.

2.5. Properties analysis of the chitosan and the natural alkali extract

2.5.1. Determination of the yield of the natural alkali: The alkali solution obtained from the ashed *E. guineensis* petiole extract was filtered, and 250 mL of the filtrate was transferred into a pre-weighed crucible and heated to dryness at 105 °C for 3 hours in an oven. It was later cooled in a desiccator, and its weight was measured on a weighing balance. The actual amount of alkali was calculated from 100 g of ash, and the extraction yield (%) was determined as given in the equation below

$$Percentage\ Yield\ (\%) = \frac{Weight\ of\ extract\ after\ evaporating\ (g)}{Dry\ weight\ of\ the\ sample\ (g)} \times 100$$

Other physical properties of chitosan, such as water and fat-binding capacities, determination yield, degree of deacetylation, and solubility in 1% acetic acid, were determined as described by Obiefuna & Chukwudum (2024).

2.6. Fourier Transform Infrared Spectroscopy (FTIR) analysis: The nano chitosan sample was characterized in KBr pellets using an infrared spectrophotometer model (4100 Jasco, Japan) in the 400-4,000 cm–1 range.

2.7. Scanning Electron Microscopy: The nanochitosan surface's morphology was examined using scanning electron microscopy (SEM) with a model (SEM-JSM 7600F, USA) having a magnification range of 9,000 and an accelerating voltage of 20 kV. Five grams of the sample were placed on a double adhesive on a sample stub, coated with a 5nm layer of gold using a sputter coater by Quorum technologies model (Q150R), and were imaged using SEM software model (Phenom ProX, by PhenomWorld, Einhoven, the Netherlands) to establish their morphological parameters.

2.8. Transmission Electron Microscopy (TEM): TEM was used to determine the particle size, size distribution, and morphology of the sample. A drop of aqueous solution of the samples was placed on the carbon-coated copper grids and dried under an infrared lamp. Micrographs were obtained using a Philips CM200 TEM operating at 200 kV.

2.9. X-ray Diffraction Spectroscopy (XRD): X-ray diffractometry measurement was carried out on the sample using an X-ray diffractometer (model: Rigaku D/Max-lllC, Tokyo, Japan) using CuKα radiation (λ = 1.540598 nm, Ni-filter) set at 40 kV and 20 mA to produce diffractions at a scanning rate of 2 0/min in the 2 to 500 ° range at room temperature. The intensity of diffracted X-rays was continuously recorded as the sample and detector rotated through their respective angles. The results were commonly presented as peak positions at 2θ and X-ray counts (intensity).

2.10. Thermal Gravimetric Analysis (TG): It was used to determine the thermal stability and decomposition temperature of the sample. The TG analysis was performed using the UW_MSE TA (model: TGA Q50) instrument. Nitrogen was used as a carrier gas at a flow rate of 50 ml min−1. The samples were heated from 30 to 600°C at a rate of 20°C/min to record the TG and differential thermogravimetry (DTG) curves.

3.0. Results and Discussion

3.1. Property and Proximate Results

Table 1.0: Properties analysis of the alkali extract of the ashed *E. guineensis*

Sample	Ash (%)	pH	Percentage yield (%)	Alkali content (mol/dm^3)
E. guineensis	17.30± **0.05**	11.74±**0.03**	76.20±**0.011**	0.88

Table 1.0 above shows the ash and alkali content of the agro-waste (*E. guineensis*) and the percentage alkali extracts. The ash content usually indicates the extent of mineral matter likely to be present in food substances. The ash content of the *E. guineensis* petiole (17.30%) was higher when compared to the findings of Romes et al. (2019), whose ash content of isolated *E. guineensis* leaves extract was 5.2%. This could be attributed to the different anatomy of the oil palm, as the petiole has more biomass than the leaf of *E. guineensis.*

The pH of 11.74 indicates that the EG petiole extract solution is strongly alkaline. Furthermore, the EG petiole extract shows an alkaline concentration of 0.88 mol/dm3 after standardisation. This result agreed with the pH of the EG petiole extract, as reflected in the alkali percentage yield obtained. The percentage alkali yield of *E. guineensis* was 76.20 %. The percentage alkali yield of *E. guineensis* was very much higher than the results obtained by Yin et al. (2017), who reported alkali percentage yields of 8.28 %, 3.08 %, and 3.10 % from *E.*

guineensis leaf extract with different solvents. The high alkali yield of *E. guineensis* petiole's extract could be attributed to the high ash content of the biomass of *E. guineensis*, since an increase in ash content increases the total alkali content (Puri et al., 2024). This makes it a better substitute for industrial caustic soda.

Table 2.0: Proximate and properties analysis of the CE

Sample	Moisture (%)	Ash (%)	Protein (%)	Fat (%)	D.D (%)	Solubility	Yield (%)	WBC (%)	FBC (%)
Chitosan (CE)	4.43 **± 0.09**	5.26 **±0.026**	1.06 **±0.003**	0.48 **±0.014**	90.55	++	89% **±0.018**	1260 **±0.06**	381.30 **±0.017**

CE = chitosan extracted using *E. guineensis* alkali extract; ++ = soluble,

Table 1.2 above shows the proximate and property values of moisture, ash, crude protein, crude fat, percentage yield, solubility, degree of deacetylation, water-binding capacity, and fat-binding capacity of chitosan from periwinkle shell waste, using *E. guineensis* alkali extract as the deacetylation and deproteination agent, as discussed below.

Moisture content: In this study, the moisture content of CE was 4.43 ± 0.09%, which was lower than that reported by Obiefuna and Chukwudum, (2024). Chitosan products should contain less than 10% moisture (Li et al., 2020). Low moisture content reduces the risk of microbial growth and degradation, helping maintain structural integrity and thereby enhancing shelf life (Gulabrao *et al*., 2024).

Ash content: CE showed that the value of the ash content was (5.26±0.026%) and higher than the values reported by Kadak et al. (2023) and Gulabrao et al. (2024), whose ash content ranged between 0.98- 1.01% and 3.33%, respectively. This shows that the chitosan prepared had a percentage of inorganic mineral residue after demineralization and could possibly be from the *Elais guineensis* alkali's extract. This could affect viscosity, solubility, and crystallinity, and may contribute to thermal stability or specific functional uses (Tertsegha et al., 2024; Mohanasrinivasan et al., 2014).

Protein and fat content: The protein and fat content values were (1.06%±0.003%) and (0.48%±0.014%), respectively, which are low when compared to the previous studies of Obiefuna and Chukwudum, (2024) and Mohanasrinivasan et al. (2014) but align with the findings of Berlin & Leena, (2022). The extracted low-fat, low-to-moderate-protein nanochitosan is suitable for many applications due to its improved hydrophilicity.

Solubility: The use of acetic acid as a solvent for dissolving chitosan and the crosslinking temperature generally affect the size distribution during dissolution (Jhaveri et al., 2021). Table 2 shows that the chitosan extracted using *Elais guineensis* alkali extract as a deacetylating agent is soluble in 1% acetic acid, consistent with existing literature and indicating good chitosan quality (Obiefuna & Chukwudum, 2024).

Percentage yield: The percentage yield of the chitosan extracted from the periwinkle waste shell was 89±0.18% using the *Elais guineensis* alkali's extract, which was higher than the percentage yield of 58% obtained by Obiefuna and Chukwudum, (2024) when commercial caustic NaOH was used to extract chitosan from periwinkle shells, but was slightly lower than that reported by Yusan et al. (2024) with a percentage yield of 90.7%.

Degree of Deacetylation (DD): Table 2.0 above shows that the DD from CE was 90.55, which is

higher than the findings of Kumari et al. (2017) and Yusan et al. (2024), i.e., (≈70- 85%), but aligns within the range of Nguyen et al. *(*2022 (≈86–92%). It indicates that the extracted chitosan has higher purity and that the acetyl group was removed during extraction. Also, CE is similar to "high-DD" chitosans used for advanced applications (Nguyen et al., 2022). High DD increases the number of $–NH_2$ groups, improves positive charge density, enhances solubility in acid, and promotes cross-linking interactions with fats and dyes (Silva et al., 2021). High alkali concentration and heating time also affect the degree of deacetylation (Tamzi et al., 2020).

Water and Fat binding capacities: The WBC and FBC contents were 1260% and 381.30%, respectively. This indicates a very hydrophilic, porous, and swollen network, likely enhanced by nanoscale size and influenced by the high Degree of Deacetylation observed earlier (Yusan et al., 2024). The WBC values obtained were higher than those reported by Berlin and Leena (2022), while the FBC content was lower than their findings but higher than those reported by Kumari et al. (2017). Fat Binding Capacity (FBC) is the ability of chitosan to interact with or adsorb fats and is a major characteristic as a food supplement (Apetroaei et al., 2019), making CE a suitable material for food, nutraceuticals, and adsorption applications.

3.2. FTIR Characterization analysis:

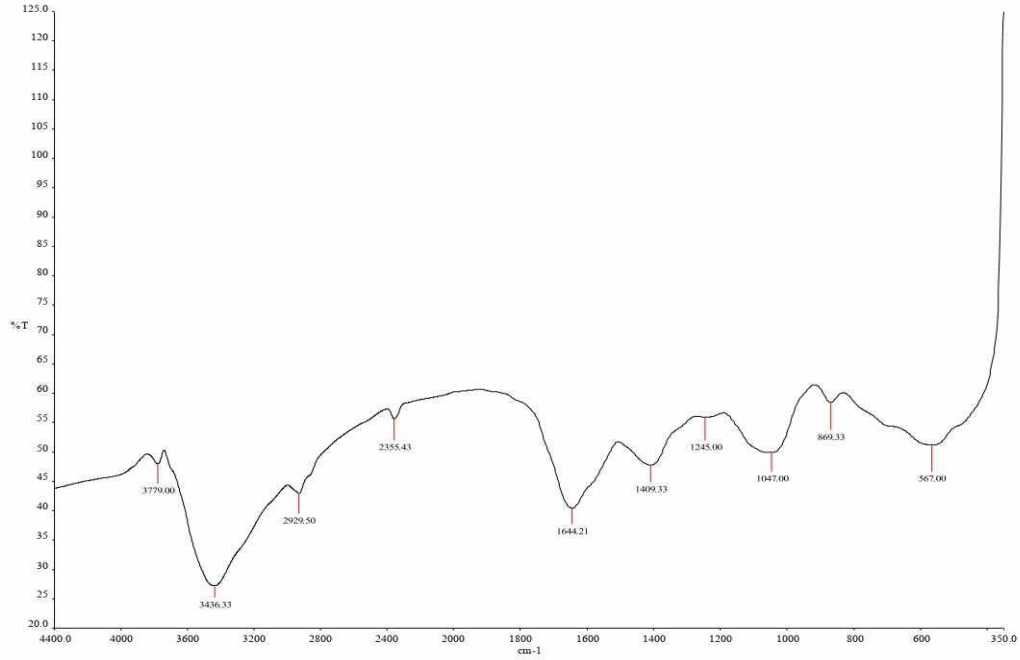


Figure 1: FTIR Spectrum of ENC

Fourier transform infrared (FTIR) spectroscopy is an analytical technique used to determine the vibration of functional groups present in nanochitosan (Obiefuna & Chukwudum, 2024). The IR spectrum of ENC (*E. guineensis* nanochitosan) as shown in Figure 1 above exhibited prominent peaks observed at approximately 3779.00cm^{-1}, 3436.33 cm^{-1}, 2929.50 cm^{-1}, 2355.43 cm^{-1}, 1644.21 cm^{-1}, 1409.33 cm^{-1}, 1047.00 cm^{-1}, 869.33 cm^{-1}, and 567.00 cm^{-1}. The results showed the presence of free hydroxyl groups (3779.00cm^{-1}), hydrogen-bonded O-H (3436.33 cm^{-1}), and N-H, which is assigned to overlapping O–H and N–H stretching vibrations of chitosan's hydroxyl and amino groups, often appearing as a broad band stretching vibrations in amines in line with Elfadl et al. (2023). Aliphatic C–H stretching of –CH_2/–CH_3 groups was observed at 2929.5 cm^{-1} in the chitosan backbone, typical near 2920–2935 cm^{-1} (Ismail *et al.,* 2023). The presence of amide at 1644.2 cm^{-1}, which corresponds to amide I (C=O stretching) of residual N-acetyl groups (CO-NH_2) and/or bound water, usually found at 1635–1660 cm^{-1} in chitosan and its nanoparticles (Pramitha et al., 2021; Kızılkaya & Kaya, 2024). CH_2/CH_3 bending was observed at 1409.3 cm^{-1}, which is usually reported in chitosan and chitosan–NP (Zam et al., 2021). The peak observed at 1047 cm^{-1} corresponds to the stretching vibrations of the C-O and C–O–C stretching bonds of the glucosamine ring and primary alcohol groups, which falls into a typical strong chitosan band near 1020–1070 cm^{-1} (Ismail et al., 2023; Pramitha et al.,2021). In addition, the peaks observed at 869 cm^{-1} and 567 cm^{-1} can be attributed to out-of-plane C-H bending vibrations, characteristic of aromatic compounds, and to C-X stretching vibrations, respectively. The FTIR spectra of ENC align with the findings of Pramitha et al. (2021), which indicated that nanochitosan was synthesized with functional groups indicating core reactive sites. The slight shifts or broadening of the peaks compared to bulk chitosan are typically due to reduced particle size, increased surface area, and altered hydrogen bonding at the nanoscale (Divya & Jisha, 2018).

3.3. Scanning Electron Microscopy (SEM) analysis:

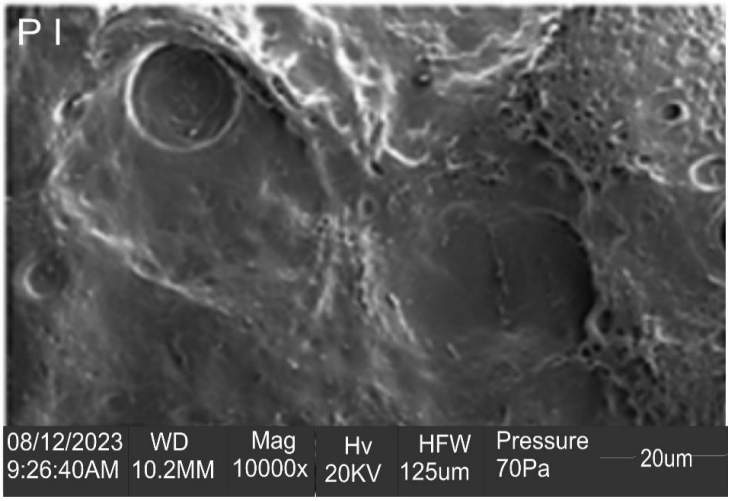


Figure 2: SEM image of ENC particle

SEM analysis, as shown in Figure 2 above, revealed that the particle was within the nanoscale range, with a surface morphology of rough, porous, agglomerated spherical particles, consistent with the findings of Okafor et al. (2024), which could result from the addition of sodium TTP, as reported by El-Naggar et al. (2022), which significantly affects the morphology of nanochitosan and particle size. Some areas of the surface exhibited a layered or stratified appearance, suggesting a potentially intricate internal structure resulting from the green extraction method used and strong intermolecular interactions during synthesis (Acay et al., 2020). This enhances surface reactivity and adsorption capacity, making the material suitable for filtration, adsorption, and use as a tissue-engineering framework (Dutta et al., 2022).

3.4. Transmission Electron Microscopy (TEM) Analysis:

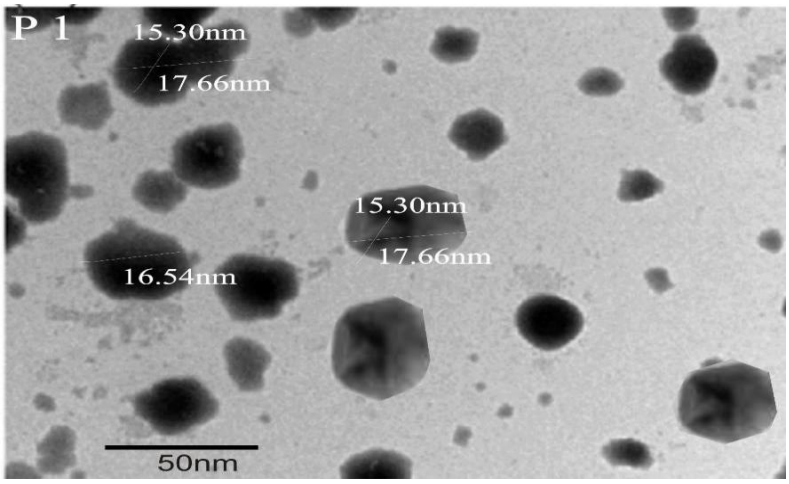


Figure 3: TEM image of ENC Particle

TEM analysis in Figure 3 above demonstrated the nanoscale structure, with particle sizes ranging from 15.30 to 17.66 nm, indicating the successful synthesis of uniform, spherical, nanoscale particles with minimal aggregation (i.e., slightly polygonal). The slightly irregular

shape could be attributed to fast nucleation during the synthesis, crosslinking, and drying process of the ENC (Cannavà et al., 2022; Lall et al., 2020). Chitosan nanoparticles imaged by TEM are generally spherical, well-distributed, and often described as having homogeneous size distributions when synthesis is well controlled (Anju et al., 2025& El-Naggar et al., 2019). The results obtained in the above TEM correspond to those of Tawfik & El-Masry (2021), whose commercial CSNPs have a diameter range of 16-25 nm after reduction achieved through the ionotropic gelation method. The diameter range obtained was lower than that reported by Aranaz et al. (2021), whose diameter ranged between 20 and 100nm. In addition, TEM results on ENC particles suggest a high surface area, which is favourable for drug loading (improved cellular uptake) and for higher adsorption efficiency in environmental and antimicrobial applications, as nanoparticles interact more effectively with microbial membranes. (Bouillons-Gamboa et al., 2024; Jha & Mayanovic, 2023).

3.5. X-ray Diffraction Analysis:

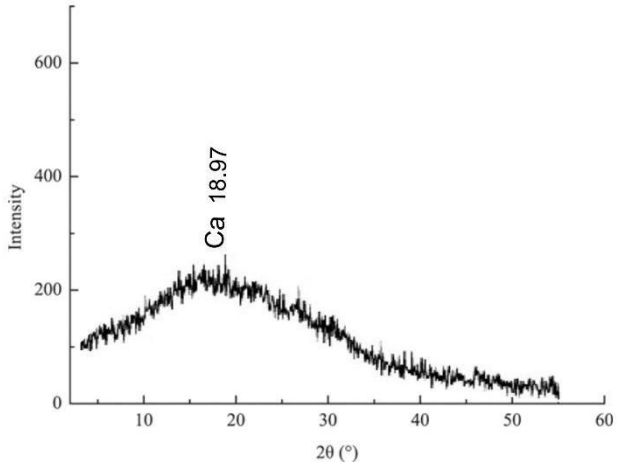


Figure 4: XRD diffractogram of ENC

It is observed from the diffractogram above in Figure 4 that the primary peak occurs around 2θ = 20°, which is similar to the pattern observed for ChN particles (Rasaee et al., 2016). The presence of this peak in the sample indicates that ENC is semi-crystalline. The presence of an additional peak indicating "Ca 18.97" at a 2θ value of 18.97° suggests that there exists a peak in the sample that corresponds to calcium. The presence of calcium possibly originated from the periwinkle shell, which is high in calcium. The presence of broad peak patterns suggests a possible decrease in crystallinity due to the breakdown of hydrogen-bonded crystalline domains, which occurs when the chitosan is reduced to the nanoscale. This aligns with findings that nanochitosan exhibits lower crystallinity than bulk chitosan, primarily due to mechanical, chemical, or ionic gelation processes used during synthesis (Divya & Jisha, 2018). The lower crystallinity improves the surface activity and solubility of nanochitosan, making it suitable for catalysis, drug delivery, and adsorption (Jampafuang et al., 2019).

Anachem Journal, 17(1), 68-81
DOI: https://doi.org/10.5281/zenodo.20129473

3.6. Thermogravimetry Analysis:

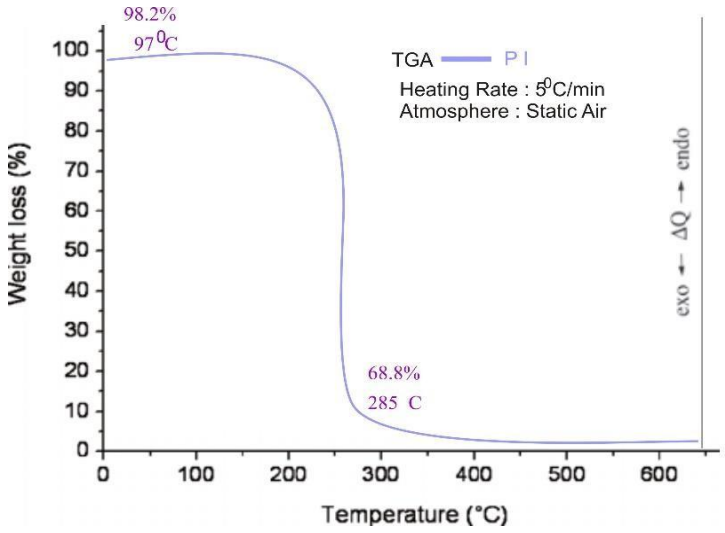


Figure 5: Thermogram of ENC

The TGA curve of the nanochitosan sample ENC represented in Figure 5 above exhibited thermal stability up to approximately 98.2% at 97°C, demonstrating negligible weight loss due to evaporation of physically and weakly bound water, not polymer degradation (Corazzari *et al.,* 2015; Iveth Saenz-Mendoza, 2023). The primary decomposition occurs at approximately 285°C, resulting in a weight loss of approximately 29.4%, corresponding to the pyrolytic degradation of the chitosan chains (Alehosseini *et al.,* 2022). The TGA findings for ENC were higher than those reported by Alehosseini et al. (2022), whose CSNP thermogram recorded ~48% mass. ENC exhibited excellent thermal stability, with minimal deterioration after exposure to 600°C.

4.0. Conclusions

The study successfully demonstrated the extraction of nanochitosan from periwinkle shells using an eco-friendly alkali source from the petiole of *E. guineensis* as a green agent for deproteination and deacetylation, resulting in higher deacetylation levels that can favorably replace industrial caustic alkali. The synthesized nanochitosan exhibited favorable physical and functional properties, indicating its strong potential for various industrial applications, especially in biomedical, food, pharmaceutical, and agricultural fields. In addition, this method can reduce raw material costs and minimise toxicity and environmental hazards during

chitosan production. Overall, this research highlighted the use of locally sourced agro-wastes for low-cost, sustainable nano-chitosan

production, thereby reducing waste and promoting environmental sustainability.

Conflict of Interest: The authors declare no conflicts of interest.

REFERENCES

Acay, H., Yıldırım, A., Güzel, E., Kaya, N., & Baran, M. (2020). Evaluation and characterization of *Pleurotus eryngii* extract-loaded chitosan nanoparticles as antimicrobial agents against some human pathogens. *Preparative Biochemistry & Biotechnology*, 50, 897-906. https://doi.org/10.1080/10826068.2020.1765376.

Agbenorku, P., Akpaloo, J., Aboah, K., Klutsey, E., Hoyte-Williams, P. E., Farhat, B., Turkson, E., Yorke, J., Ametih, R., & Hussey, R. (2015). Chemical burn injury in Kumasi: the trend and complications following and their management. *Plastic and Reconstructive Surgery–Global Open*, 3(10), e548.

Alehosseini, E., Shahiri Tabarestani, H., Kharazmi, M. S., & Jafari, S. M. (2022). Physicochemical, thermal, and morphological properties of chitosan nanoparticles produced by ionic gelation. *Foods*, 11(23), 3841.

Anju, A., Gopal, K., Panchami, P., Vijayaraghavan, R., & Nano, D. (2025). A simple and user-friendly protocol for chitosan nanoparticle synthesis. *Discover Nano,* 20(1). https://doi.org/10.1186/s11671-025-04391-8.

Apetroaei, M. R., Rau, I., Paduretu, C. C., Lilios, G., & Schroder, V. (2019). Pharmaceutical applications of chitosan extracted from local marine sources. *Rev. Chim*, 70, 2618-2621.

Aranaz, I., Alcántara, A. R., Civera, M. C., Arias, C., Elorza, B., Heras Caballero, A., & Acosta, N. (2021). Chitosan: An overview of its properties and applications. *Polymers*,13(19), 3256

Berlin, M., & Leena, R. (2022). Extraction and Characterization of Chitin and Chitosan from Penaeus Monodon and its Application for Water Purification: An Approach to Utilize Waste. *Current World Environment, 17(3)*. https://doi.org/10.12944/cwe.17.3.24.

Bouillons-Gamboa, R., De Oca, G., Baudrit, J., Duarte, L., Lopretti, M., Urquiza, M., Zúñiga-Umaña, J., Barreiro, F., & Vázquez, P. (2024). Synthesis of chitosan nanoparticles (CSNP): effect of CH-CH-TPP ratio on size and stability of NPs. Frontiers in Chemistry, 12. https://doi.org/10.3389/fchem.2024.1469271.

Cannavà, C., De Gaetano, F., Stancanelli, R., Venuti, V., Paladini, G., Caridi, F., Ghica, C., Crupi, V., Majolino, D., Ferlazzo, G., Tommasini, S., & Ventura, C. (2022). Chitosan-Hyaluronan Nanoparticles for Vinblastine Sulfate Delivery: Characterization and Internalization Studies on K-562 Cells. *Pharmaceutics,* 14(5). https://doi.org/10.3390/pharmaceutics14050942.

Corazzari, I., Nisticò, R., Turci, F., Faga, M., Franzoso, F., Tabasso, S., & Magnacca, G. (2015). Advanced physico-chemical characterization of chitosan by means of TGA coupled on-line with FTIR and GCMS: Thermal degradation and water adsorption capacity. *Polymer Degradation and Stability,* 112, 1-9. https://doi.org/10.1016/j.polymdegradstab.2014.12.006.

Divya, K., & Jisha, M. S. (2018). Chitosan nanoparticles preparation and applications. *Environmental chemistry letters,* 16(1), 101-112.

Dutta, P., Kumari, A., & Mahanta, M. (2022). Chitosan nanoparticle: synthesis, characterization, and use as plant health materials. In Chitin and chitosan-isolation, properties, and applications. *IntechOpen.*

Elfadl, A., Bashal, A., Habeeb, T., Khalafalla, M., Alkayal, N., & Khalil, K. (2023). Preparation, Characterization, Dielectric

Properties, and AC Conductivity of Chitosan Stabilized Metallic Oxides CoO and SrO: Experiments and Tight Binding Calculations. *Polymers,* 15. https://doi.org/10.3390/polym15204132.

El-Naggar, M. M., Abou-Elmagd, W. S., Suloma, A., El-Shabaka, H. A., Khalil, M. T., & Abd El-Rahman, F. A. (2019). Optimization and physicochemical characterization of chitosan and chitosan nanoparticles extracted from the crayfish Procambarus clarkii wastes. *Journal of Shellfish Research*, 38(2), 385-395.

El-Naggar, N., Shiha, A., Mahrous, H., & Mohammed, A. (2022). Green synthesis of chitosan nanoparticles, optimization, characterization and antibacterial efficacy against multi drug resistant biofilm-forming Acinetobacter baumannii. *Scientific Reports,* 12. https://doi.org/10.1038/s41598-022-24303-5.

El-Saadony, M., Saad, A., Sitohy, M., Alkafaas, S., Dladla, M., Ghosh, S., Mohammed, D., Soliman, T., Ibrahim, E., Fahmy, M., Qamar, J., & Tarabily, K. (2025). Chitosan nanoparticles: Green synthesis, biological activities, and sustainable frontiers in targeted drug delivery and cancer nanomedicine – A comprehensive review. *Materials Today Bio,* 35. https://doi.org/10.1016/j.mtbio.2025.102358.

Gbenebor, O. P., Akpan, E. I., & Adeosun, S. O. (2017). Thermal, structural and acetylation behavior of snail and periwinkle shells chitin. *Progress in biomaterials*, 6(3), 97-111.

Gulabrao, D., Amarnatha, N., Reddy, H., D., T., M., K., & Reddy, N. (2024). Physicochemical Properties of Chitosan Extracted from Silkworm (Bombyx mori L.) Exuviae. *Journal of Advances in Biology & Biotechnology*. https://doi.org/10.9734/jabb/2024/v27i81263.

Ismail, A., M.Tiama, T., Farghaly, A., Elhaes, H., & Ibrahim, M. (2023). Assessment of the Functionalization of Chitosan/ Iron Oxide Nanoparticles. *Biointerface Research in Applied Chemistry.* https://doi.org/10.33263/briac136.582.

Iveth Saenz-Mendoza, A., Baruk Zamudio-Flores, P., Manuel Tirado-Gallegos, J., Cristina García-Anaya, M., Rios Velasco, C., Horacio Acosta-Muñiz, C., Espino-Díaz, M., Hernández-González, M.,Vela-Gutiérrez, G., Salgado-Delgado, R., Rendón-Villalobos & Ortega-Ortega, A. (2023). Insects as a potential source of chitin and chitosan: Physicochemical, morphological and structural characterization.-A review. *Emirates Journal of Food & Agriculture (EJFA),* 35(5).

Jampafuang, Y., Tongta, A., & Waiprib, Y. (2019). Impact of Crystalline Structural Differences Between α- and β-Chitosan on Their Nanoparticle Formation Via Ionic Gelation and Superoxide Radical Scavenging Activities. *Polymers,* 11. https://doi.org/10.3390/polym11122010.

Jha, R., & Mayanovic, R. (2023). A Review of the Preparation, Characterization, and Applications of Chitosan Nanoparticles in Nanomedicine. *Nanomaterials*, 13. https://doi.org/10.3390/nano13081302.

Jhaveri, J., Raichura, Z., Khan, T., Momin, M., & Omri, A. (2021). Chitosan nanoparticles-insight into properties, functionalization and applications in drug delivery and theranostics. *Molecules,* 26(2), 272.

Kızılkaya, P., & Kaya, M. (2024). Chitosan/TiO2/Rosmarinic Acid Bio-Nanocomposite Coatings: Characterization and Preparation. *Journal of Composites Science*. https://doi.org/10.3390/jcs9010002.

Kumari, S., Annamareddy, S. H. K., Abanti, S., & Rath, P. K. (2017). Physicochemical properties and characterization of chitosan synthesized from fish scales, crab and shrimp shells. *International journal of biological macromolecules*, 104, 1697-1705.

Lall, A., Tamo, A., Doench, I., David, L., De Oliveira, P., Gorzelanny, C., & Osorio-Madrazo, A. (2020). Nanoparticles and Colloidal Hydrogels of Chitosan–Caseinate Polyelectrolyte Complexes for Drug-Controlled

Release Applications. *International Journal of Molecular Sciences,* 21. https://doi.org/10.3390/ijms21165602.

Li, Q., Dunn, E. T., Grandmaison, E. W., & Goosen, M. F. (2020). Applications and properties of chitosan. In Applications of Chitan and Chitosan (pp. 3-29). CRC Press.

Maliki, M., Ifijen, I. H., & Omorogbe, S. O. (2020). Cocoa husks: a sustainable resource for alkali production. *International Journal of Biological and Chemical Sciences*, 14(7), 2652-2658.

Mohanasrinivasan, V., Mishra, M., Paliwal, J. S., Singh, S. K., Selvarajan, E., Suganthi, V., & Subathra Devi, C. (2014). Studies on heavy metal removal efficiency and antibacterial activity of chitosan prepared from shrimp shell waste. *Biotech*, 4(2), 167-175.

Nguyen, H., Tran, T., Ha, A., & Huynh, P. (2022). Impact of Deacetylation Degree on Properties of Chitosan for Formation of Electrosprayed Nanoparticles. *Journal of Nanotechnology*. https://doi.org/10.1155/2022/2288892.

Obiefuna, J. N., & Chukwudum, J. I. (2024). Comparative Studies of the Physicochemical Properties of Chitosan from Commercial and Locally Sourced Periwinkle Shell from Akwa-Ibom. *ANACHEM Journal*, 15(1), 16-26.

Okafor, V., & Obiefuna, J. (2024). Comparative studies of the physicochemical properties of chitosan from commercial and biowaste sources. *Journal of Basic Physical Research,* 12(2), 89-97.

Okafor,V. Nwalieji, Kehinde,D. Oluwalana, Akinyele,A. Bankole and Modozie,B. Uchenna (2024). Synthesis of Nanochitosan from Cambarus Bartonii Waste and its Utilization in the Removal of Polycyclic Aromatic Hydrocarbons in Surface Water from Ifite Ogwari, Southeastern Nigeria. *Nanochemistry Research*, 9(1), 42-54. doi: 10.22036/NCR.2024.01.06

Okolo, C. C., Okolo, E. C., Nnadi, A. L., Obikwelu, F. E., Obalum, S. E., & Igwe, C. A. (2019). The oil palm (*Elaeis guineensis* Jacq): nature's ecological endowment to eastern Nigeria. *Agro-Science*, 18(3), 48-57.

Pramitha, V., Sajeetha, S., Alsif, H., Aiswarya, A., Fathima, J., Beegumsahina, S., & Aryaraj, D. (2021). Characterization and Bioactivity Study of Chitosan Based Nanomaterial from Exoskeleton Waste of *Parapaeneopsis Stylifera.* . https://doi.org/10.21203/rs.3.rs-508681/v1.

Puri, L., Hu, Y., & Naterer, G. (2024). Critical review of the role of ash content and composition in biomass pyrolysis. *Frontiers in Fuels*, 2, 1378361

Rasaee, I., Ghannadnia, M., & Honari, H. (2016). Antibacterial properties of biologically formed chitosan nanoparticles using aqueous leaf extract of *Ocimum basilicum. Nanomed* J, 3(4), 240-247.

Riki, R., Ahmad, I., Herman, H., Ibrahim, A., Rusman, A., Samsul, E., Rusli, R., Arifuddin, M., Junaidin, J., Bone, M., Rijai, H., & Hikmawan, B. (2025). An Innovative Strategy for the Green Synthesis of Nanochitosan Using Plant Extracts and Their Possible Applications: A Review. *Indonesian Journal of Chemistry*. https://doi.org/10.22146/ijc.100148.

Romes, N. B., Wahab, R. A., & Hamid, M. A. (2019, September). Proximate analysis and bioactivity study on acoustically isolated *Elaeis guineensis* leaves extract. In AIP conference proceedings (Vol. 2155, No. 1, p. 020001). AIP Publishing LLC.

Silva, F., Gasparrini, L., Cremonez, P., Burin, G., Machado, B., Polinarski, M., Arantes, M., & Alves, H. (2021). Chitosan preparations with improved fat-binding capacity. *Journal of Applied Polymer Science,* 50841. https://doi.org/10.1002/app.50841.

Tamzi, N. N., Faisal, M., Sultana, T., & Ghosh, S. K. (2020). Extraction and properties evaluation of chitin and chitosan prepared from

different crustacean waste. *Bangladesh Journal of Veterinary and Animal Sciences,*8(2), 69-76.

Tawfik, T. M., & El-Masry, A. M. (2021). Preparation of chitosan nanoparticles and its utilization as novel powerful enhancer for both dyeing properties and antimicrobial activity of cotton fabrics. *Biointerface Res. Appl. Chem*, 11, 13652-13666.

Tertsegha, S., Akubor, P., Iordekighir, A., Christopher, K., & Okike, O. (2024). Extraction and Characterization of Chitosan from Snail Shells (Achatina fulica). *Journal of Food Quality and Hazards Control.* https://doi.org/10.18502/jfqhc.11.3.16590.

Thambiliyagodage, C., Jayanetti, M., Mendis, A., Ekanayake, G., Liyanaarachchi, H., & Vigneswaran, S. (2023). Recent advances in chitosan-based applications—a review. *Materials,* 16(5), 2073.

Vega-Baudrit, J. R., Lopretti, M., Montes de Oca, G., Camacho, M., Batista, D., Corrales, Y., Araya, A., Bahloul, B., Corvis, Y., & Castillo-Henríquez, L. (2025). Nanochitin and nanochitosan in pharmaceutical applications: Innovations, applications, and future perspective. *Pharmaceutics,* 17(5), 576.

Widiputri, D., Ayuyasmin, F., & Legowo, E. (2022). Biopellet Production from the Wastes of Palm Oil Plantation and Processing Plant Through Various Pretreatment Processes: A Review. *Advances in Biological Sciences Research*. https://doi.org/10.2991/absr.k.220101.007.

Yin, N. S., Abdullah, S., and Phin, C. K. (2013). Phytochemical constituents from leaves of Elaeis guineensis and their antioxidant and antimicrobial activities. *Int J Pharm Pharm Sci,* 5(4), 137- 140.

Yusan, L., Nailufa, Y., & Subagio, H. (2024). Isolation and characterization of chitosan nanoparticles from crab shell waste (*portunus pelagicus*). *International Journal of Applied Pharmaceutics*. https://doi.org/10.22159/ijap.2024v16i2.49638.

Zam, Z., Muin, F., & Fataruba, A. (2021). Identification of chitosan beads from coconut crab patani variety using Fourier Transform Infrared Spectroscopy (FTIR). *Journal of Physics: Conference Series,* 1832. https://doi.org/10.1088/1742-6596/1832/1/012014.